Hydrogen/silicon complexes in silicon from computational searches

Andrew J. Morris,[1,*] Chris J. Pickard,[2] and R. J. Needs[1]

[1]*Theory of Condensed Matter Group, Cavendish Laboratory, University of Cambridge, J. J. Thomson Avenue, Cambridge CB3 0HE, United Kingdom*

[2]*Scottish Universities Physics Alliance, School of Physics and Astronomy, University of St. Andrews, North Haugh, St. Andrews KY16 9SS, United Kingdom*

Defects in crystalline silicon consisting of a silicon self-interstitial atom and one, two, three, or four hydrogen atoms are studied within density-functional theory (DFT). We search for low-energy defects by starting from an ensemble of structures in which the atomic positions in the defect region have been randomized. We then relax each structure to a minimum in the energy. We find a new defect consisting of a self-interstitial and one hydrogen atom (denoted by $\{I, H\}$) which has a higher symmetry and a lower energy than previously reported structures. We recover the $\{I, H_2\}$ defect found in previous studies and confirm that it is the most stable such defect. Our best $\{I, H_3\}$ defect has a slightly different structure and lower energy than the one previously reported, and our lowest-energy $\{I, H_4\}$ defect is different to those of previous studies.

I. INTRODUCTION

Hydrogen is a very common impurity in semiconductors whose roles in silicon include passivating surfaces and defects.[1] Much is known about the vacancy in silicon but rather little understanding of self-interstitials has been gleaned from experiments, so there is considerable reliance on theoretical work. Self-interstitials are common in silicon and they are expected to react with impurities to form defect complexes. Mobile hydrogen atoms are expected to bind strongly to self-interstitial defects in silicon, and hydrogen-silicon complexes have been detected in experiments.[2]

Silicon self-interstitials are readily formed during device manufacture and bombardment with electrons or ions. According to DFT calculations, the most stable structure is the split-$\langle 110 \rangle$ defect, with the hexagonal interstitial being slightly higher in energy and the tetrahedral interstitial being still higher in energy.[3–5] The results of two quantum Monte Carlo calculations are consistent with these three defects having low energies.[3,6] Mukashev *et al.*[7] attributed the AA12 electron-paramagnetic-resonance center to a self-interstitial defect, possibly a single self-interstitial. Calculations by Eberlein *et al.*[8] found the doubly-positively-charged single self-interstitial to be stable at the tetrahedral site, and that it was broadly consistent with the AA12 defect.

Much of what is known about hydrogen in silicon has been learned from studies of vibrational modes which are accessible to infrared-absorption experiments and may also be calculated within first-principles methods. Only one hydrogen-silicon complex has so far been firmly identified in experiments. Budde *et al.*[2] identified the silicon self-interstitial with two hydrogen atoms using Fourier transform infrared (FTIR) absorption spectroscopy. The observed properties were found to be in excellent agreement with the results of DFT calculations.[2]

Throughout this paper we denote the silicon self-interstitial atom by I and the n hydrogen atoms by H_n, and the whole defect is referred to as $\{I, H_n\}$. A metastable defect is indicated by an asterisk. We also use the notation devised by Gharaibeh *et al.*[9] where (n)-$(m)\cdots$ means n hydrogen atoms bonded to one silicon atom and m hydrogen atoms bound to a neighboring silicon atom, etc. For example, the silicon self-interstitial bonded to two hydrogen atoms mentioned above is referred to as $\{I, H_2\}$ and the arrangement of H atoms shown in Fig. 4 is described as (1)-(1).

The first calculations we are aware of on the $\{I, H\}$ defect were by Déak *et al.*,[10] who reported two possible structures which, however, are different from those found subsequently by Van de Walle and Neugebauer.[11] In each structure found by Déak *et al.*[10] the second-nearest-neighbor silicon atom to the hydrogen has a dangling bond, whereas the lowest-energy structure of Van de Walle and Neugebauer[11] does not contain dangling bonds. Budde *et al.*[2] found $\{I, H\}$ structures based on split-$\langle 110 \rangle$ and split-$\langle 100 \rangle$ self-interstitials both of C_{1h} symmetry, with the $\langle 110 \rangle$ defect being 0.24 eV lower in energy. The $\{I, H\}$ defect based on the split-$\langle 110 \rangle$ interstitial was similar to that found by Van de Walle and Neugebauer[11] whereas the split-$\langle 100 \rangle$ is similar to the lowest-energy structure of Déak *et al.*[10] Gharaibeh *et al.*[9] found a structure similar to lowest-energy defect of Van de Walle and Neugebauer.[11]

Déak *et al.*[10,12] also studied the $\{I, H_2\}$ defect. Their lowest-energy $\{I, H_2\}$ defect is also based on a split-$\langle 110 \rangle$ self-interstitial with its two dangling bonds terminated by hydrogen atoms. Further evidence in favor of this structure has been obtained in a variety of studies.[2,9,11,13] Gharaibeh *et al.*[9] also found this to be the most stable of the $\{I, H_n\}$ family of defects.

Hastings *et al.*[13] studied the $\{I, H_3\}$ defect within Hartree-Fock (HF) theory, finding a structure with two hydrogen atoms bonded to a silicon and a third bonded to a neighboring silicon, i.e., a (2)-(1) configuration of hydrogen atoms. They found interstitial silyl (SiH$_3$) to be 0.44 eV higher in energy and concluded that it is unlikely to be found in bulk silicon. More complete DFT calculations by the same group[9] found a $\{I, H_3\}$ defect with a (1)-(1)-(1) configuration.

Hastings *et al.*[13] studied the $\{I, H_4\}$ defect within HF theory, finding a ground-state structure similar to the $\{I, H_2\}$ defect, but with additional hydrogen atoms bonded to the

nearest-neighbor and second-nearest-neighbor silicon atoms to the self-interstitial, resulting in a (1)-(1)-(1)-(1) configuration. They also found a metastable (2)-(2) configuration 0.2 eV higher in energy and showed that interstitial silane (SiH_4) is very unlikely to form. A later DFT study by the same group[9] found the ground state of $\{I, H_4\}$ to be a (3)-(1) configuration.

In this paper we present calculations for the defects $\{I, H_i\}$, $i = 1, 4$, as found by a "random structure searching" approach using first-principles DFT methods. We describe the random structure searching scheme in Sec. II A. The nonstandard Brillouin-zone (BZ) integration scheme we have used is described in Sec. II B, and the details of our DFT calculations and some convergence tests are reported in Sec. II C. Our results are described in Sec. IV and our main conclusions are summarized and discussed in Sec. V.

II. COMPUTATIONAL APPROACH

A. Random structure searching

"Random structure searching" has already proven to be a powerful tool for finding structures of solids under high pressures.[14–19] The basic algorithm is very simple: we take a population of random structures and relax them. This approach is surprisingly successful and its performance for large systems can be improved by imposing constraints. The constraints we have typically employed in work on high-pressure phases are to (i) choose the initial positions of a local minimum and randomly displace the atoms by a small amount, (ii) insert "chemical units" (for example molecules) at random rather than atoms, (iii) search within structures of a particular symmetry, and (iv) constrain the initial positions of some atoms.

Pickard and Needs[14] showed that "random structure searching" can be applied to finding structures of point defects. In the current work we have searched for silicon self-interstitial defect structures using a 32-atom body-centered-cubic unit cell of diamond-structure silicon. The initial configurations were generated by removing an atom and its four nearest neighbors, making a "hole" in the crystal, and placing six silicon atoms at random positions within the hole. The initial configurations therefore consisted of a region of perfect crystal and a defect region in which atoms are positioned randomly. This is an example of a constraint of type (iv) mentioned above. Relaxing the members of an ensemble of such initial configurations generated the split-⟨110⟩, tetrahedral, and hexagonal interstitial configurations, which various DFT calculations have shown to be lowest in energy.[2,4,5,20,21]

We explored four choices of the hole used to generate the initial configurations: (a) remove one silicon atom and its four nearest neighbors; (b) remove one silicon atom; (c) do not remove any silicon atoms and take the center of the hole to lie at the hexagonal site; (d) the same as (c) but with the hole at the tetrahedral site. The initial configurations were generated by placing the appropriate atoms randomly within cubic boxes of sizes ranging from 2 to 6 Å centered on the hole. Choices (b), (c), and (d) generally led to us finding the structure we believe to be most stable within roughly 100

configurations, while the larger hole of choice (a) was less successful and sometimes failed to find the ground state within 500 configurations.

B. Brillouin zone sampling scheme

The importance of performing accurate Brillouin-zone integrations when calculating defect formation energies has been emphasized by, among others, Shim *et al.*[22] DFT calculations by Gharaibeh *et al.*[9] explored the convergence of BZ sampling for self-interstitial-hydrogen complexes in silicon. Instead of standard Monkhorst-Pack (MP) sampling[23] we have used the multi-k-point generalization of the Baldereschi mean-value point scheme[24] outlined by Rajagopal *et al.*[25,26] Three linearly-independent reciprocal-lattice vectors $(\mathbf{b}_1, \mathbf{b}_2, \mathbf{b}_3)$ are chosen, which need not be primitive, and a $l \times m \times n$ grid of k-points is defined by

$$\mathbf{k}_{ijk} = \frac{i\mathbf{b}_1}{l} + \frac{j\mathbf{b}_2}{m} + \frac{k\mathbf{b}_3}{n} + \mathbf{k}_B(l,m,n), \qquad (1)$$

where

$$i = 0, 1, \ldots, l-1; \quad j = 0, 1, \ldots, m-1; \quad k = 0, 1, \ldots, n-1. \qquad (2)$$

The standard Baldereschi mean-value point[24] can be written in terms of the $\mathbf{b}_i$

$$\mathbf{k}_B = \alpha_1 \mathbf{b}_1 + \alpha_2 \mathbf{b}_2 + \alpha_3 \mathbf{b}_3, \qquad (3)$$

which defines the α_i, and the offset $\mathbf{k}_B(l,m,n)$ for the multi-k-point scheme[25,26] is

$$\mathbf{k}_B(l,m,n) = \frac{\alpha_1 \mathbf{b}_1}{l} + \frac{\alpha_2 \mathbf{b}_2}{m} + \frac{\alpha_3 \mathbf{b}_3}{n}. \qquad (4)$$

This is the natural multi-k-point generalization of Baldereschi's scheme as it corresponds to sampling the Baldereschi mean-value point of the supercell obtained by choosing direct (real-space) lattice vectors $(l\mathbf{a}_1, m\mathbf{a}_2, n\mathbf{a}_3)$, where the $\mathbf{a}_i$ are related to the $\mathbf{b}_i$ by the standard dual transformation. We will refer to this as the multi-B scheme.

In Fig. 1 we report a comparison for bulk silicon of standard $n \times n \times n$ Monkhorst-Pack grids, the same grids but centered on $\mathbf{k} = 0$ (multi-Γ), and the multi-B scheme. For odd values of n the MP and multi-Γ grids are the same, although we could of course introduce an appropriate shift of the MP grid for odd n which gives smooth convergence. The MP scheme gives smaller errors than the multi-Γ scheme for even n. The multi-B energies converge smoothly with n and give the smallest errors for each value of n.

The cost of a BZ integration is determined not by n but by the number of symmetry inequivalent k-points in the grid and the most efficient k-point grid generally depends on the symmetry of the structure. Symmetric structures normally have more inequivalent k-points in the multi-B grid than in the corresponding MP grid. During the search stage, symmetry is not imposed and we use all n^3 grid points, and therefore the multi-B scheme is the most efficient. We have used the multi-B grid in all searches reported here.
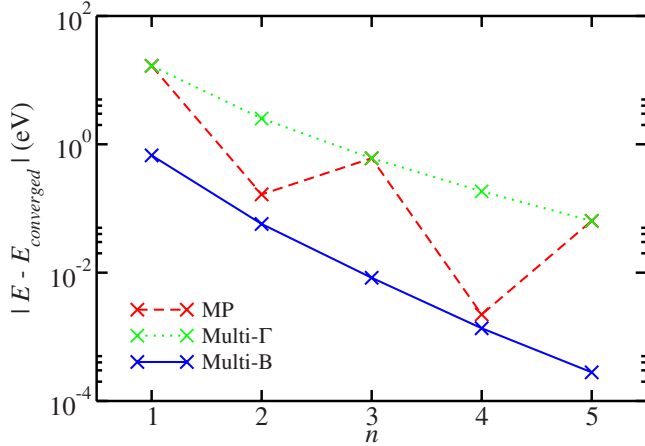
FIG. 1. (Color online) Magnitudes of the energy differences between the converged energy (taken from a multi-B calculation with $n=20$) and energies obtained with different k-point grids for a two-atom cell of diamond-structure silicon. The energies are in eV per cell and the number of points in each grid is n^3. The standard Monkhorst-Pack grid, labeled MP, is shown in red (dashed line), multi-Γ denotes grids centered on $\mathbf{k}=0$ shown in green (dotted line), and multi-B denotes the multi-k-point generalization of the Baldereschi scheme is shown in blue (solid line).

C. Density-functional theory calculations

Our calculations were performed using the generalized gradient approximation (GGA) density functional of Perdew, Burke, and Ernzerhof (PBE).[27] The plane-wave basis-set code CASTEP (Ref. [28]) was used with its built-in ultrasoft[29] pseudopotentials which include nonlinear core corrections.[30] All of the results presented here were obtained with non-spin-polarized calculations. Some searches and large supercell calculations were repeated allowing spin polarization, but no significant changes were found in the energy differences between structures. All of our calculations are for neutral unit cells.

We carried out convergence tests on the formation energy of a bond-centered hydrogen atom in silicon from interstitial H$_2$ using 256-atom silicon cells. We chose these systems because they contain very different bonding arrangements (H$_{bc}$ contains Si-Si and Si-H bonds while the H$_2$ system contains Si-Si and H-H bonds). Hence the estimates of convergence of the energy difference between these two systems should give a reasonable indication of the convergence of the energy differences between other defects. The formation energy, E_F, of a bond-centered H in silicon from interstitial H$_2$ calculated with N-atom silicon cells is

$$E_F(\mathrm{H_{bc}}, N) = E(\mathrm{H_{bc}}, N) - \frac{E(\mathrm{H_2}, N)}{2} - \frac{E(N)}{2}, \quad (5)$$

where $E(\mathrm{X}, N)$ is the energy of the X defect in a N-atom silicon cell, and $E(N)$ is the bulk energy for N atoms.

The Fourier transform grid used for wave-function manipulation was set to integrate, without aliasing, frequencies twice as high as the maximum frequency in the basis set. We checked the convergence of $E_F(\mathrm{H_{bc}})$ with respect to the charge augmentation grid required for the ultrasoft pseudo-

TABLE I. Formation energies for self-interstitial defects in 256-atom cells of silicon, as defined by Eq. (6).

Defect	$E_F(\{I\})$ (eV)
Split-$\langle 110 \rangle$	3.66
Hexagonal	3.69
Tetrahedral	3.96

potentials, finding it to be converged to within 0.005 eV at 2.75 times the maximum frequency in the orbital basis set. We found that $E_F(\mathrm{H_{bc}})$ was converged to within ± 0.02 eV with a basis set of $E_{PW}=230$ eV.

We tested different k-point sampling schemes in the 256-atom cell. The values of $E_F(\mathrm{H_{bc}})$ for the $n=3$ standard MP and multi-B grids agreed to within 0.002 eV and we therefore considered these converged. The value of $E_F(\mathrm{H_{bc}})$ calculated for the 256-atom cell with the $n=2$ standard MP grid differed from the converged result by ~ 0.04 eV, whereas the error from the multi-B grid was six-times smaller.

III. CALCULATING THE FORMATION ENERGIES

The searches were performed using a body-centered-cubic supercell of a size to contain 32-atoms of bulk silicon. We used a $n=2$ multi-B k-point grid, which we estimate gives energy differences between structures converged to within 0.006 eV. However, the 32-atom cell is too small to give highly accurate geometries and formation energies. We therefore embedded the most promising structures within 256-atom body-centered-cubic unit cells and relaxed using a $n=2$ multi-B grid until the forces on each atom were less than 0.001 eV Å^{-1}.

The formation energy of the self-interstitial is defined as

$$E_F(\{I\}, N) = E(\{I\}, N) - \frac{N+1}{N} E(N), \quad (6)$$

where $E(\{I\}, N)$ is the energy of the self-interstitial cell.

We define the formation energy per hydrogen atom of a system containing a defect with n hydrogen atoms and i silicon atoms relative to a system containing i isolated self-interstitial defects and $n/2$ interstitial hydrogen molecules as

$$E_F(\{I_i, \mathrm{H}_n\}, N) = \frac{E(\{I_i, \mathrm{H}_n\}, N) - E(\{I_i\}, N)}{n} + \frac{E(N) - E(\mathrm{H_2}, N)}{2}. \quad (7)$$

Note that Eq. (7) with $i=0$ and $n=1$ gives Eq. (5) for the formation energy of bond-centered hydrogen.

IV. RESULTS

The formation energies of self-interstitial defects as defined by Eq. (6) are given in Table I. In agreement with numerous previous studies (e.g., Refs. [2], [4], [5], [21], and [20]) we find the most stable defect to be the split-$\langle 110 \rangle$ interstitial. The hexagonal and tetrahedral interstitials are 0.03 and 0.3 eV higher in energy, respectively. Hence all three self-

TABLE II. Formation energies per H atom and degeneracies per atomic site, d_i, of hydrogen defects in silicon. The H_2 is the lowest in energy defect.

Defect	Configuration	E_F per H atom (eV)	Degeneracy d_i
H_2	Molecule	0.00	3
H_2^*	(1)-(1)	0.10	
H_{bc}	Bond center	1.04	

interstitial defects are candidates for forming a low-energy $\{I, H_n\}$ defect in the presence of hydrogen.

Our search for hydrogen defects in bulk silicon found the lowest-energy defects known previously, but no new defects were found. We found the bond-centered H atom, the H_2 molecule with the H-H bond pointing along a $\langle 100 \rangle$ direction, and the H_2^* metastable defect of Chang and Chadi.[31] The formation energies of hydrogen defects in silicon given in Table II show the H_2 molecule to be the most stable, as found in previous calculations,[32–34] with the H_2^* defect and bond-centered hydrogen being, respectively, 0.10 and 1.04 eV per H atom higher in energy.

The formation energies of the hydrogen/silicon self-interstitial complexes are calculated with reference to a system containing the most stable self-interstitial (the split-$\langle 110 \rangle$) and the most stable hydrogen defect in pure silicon, the H_2 molecule. The data in Table III show that the $\{I, H_2\}$ defect has the lowest formation energy, followed by the $\{I, H_2\}^*$. These data are shown in pictorial form in Fig. 2.

Our searches for the $\{I, H\}$ defect found the previously known structure[9,11] of C_s symmetry, but we also found a new lower-energy structure of higher C_{3v} symmetry. The C_{3v} defect, shown in Fig. 3, is 0.14 eV lower in energy and is based on a hydrogen atom bonded to a hexagonal self-interstitial with the Si-H bond pointing along a $\langle 111 \rangle$ direction, rather than the split-$\langle 110 \rangle$ interstitial on which the C_s $\{I, H\}$ defect is based.

Our searches found the $\{I, H_2\}$ (1)-(1) defect structure reported previously[2,9–13] which is shown in Fig. 4 and whose formation energy we calculated to be -0.69 eV/H. The second most stable $\{I, H_2\}$ defect, which has a (2) structure, is

TABLE III. Formation energies per H atom as defined by Eq. (7) and degeneracies per atomic site, d_i, for various hydrogen/silicon self-interstitial complexes. The formation energies are represented pictorially in Fig. 2.

Defect	Configuration	E_F per H atom (eV)	Degeneracy d_i
$\{I, H\}$	(1)	-0.53	4
$\{I, H\}^*$	(1)	-0.39	
$\{I, H_2\}$	(1)-(1)	-0.69	12
$\{I, H_2\}^*$	(2)	-0.61	
$\{I, H_3\}$	(2)-(1)	-0.39	24
$\{I, H_3\}^*$	(1)-(1)-(1)	-0.34	
$\{I, H_4\}$	(2)-(1)-(1)	-0.48	24

Formation energy per H atom (eV)
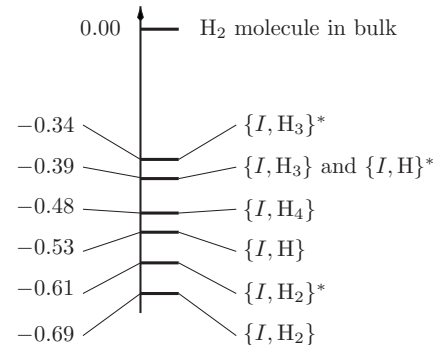
FIG. 2. Formation energies per hydrogen atom using Eq. (7) for various hydrogen defects in silicon calculated with respect to silicon containing a self-interstitial defect and silicon containing hydrogen molecules.

the $\{I, H_2\}^*$ defect found previously by Déak *et al.*[10] and is shown in Fig. 5. This defect is based on a buckled bond-centered Si atom with two H atoms saturating its dangling bonds. The $\{I, H_2\}$ and $\{I, H_2\}^*$ both have C_2 symmetry. Hastings *et al.*[13] found $\{I, H_2\}^*$ to be 0.40 eV higher in energy than $\{I, H_2\}$ within HF theory. Later, Gharaibeh *et al.*[9] found it to be 0.05 eV above the ground state. Our calculations gave an energy 0.08 eV/H higher than the $\{I, H_2\}$ of Fig. 4.

The lowest-energy $\{I, H_3\}$ defect we found is a (2)-(1) configuration of C_1 symmetry, which is shown in Fig. 6 and has a formation energy of -0.39 eV/H. This defect has the same configuration of hydrogen atoms but a different structure to the one found by Hastings *et al.*[13] using HF theory. They also found a metastable $\{I, H_3\}^*$ structure of C_1 symmetry with a (1)-(1)-(1) configuration just 0.1 eV higher in energy. However, more recently this group have used DFT methods and found the (1)-(1)-(1) configuration to be lower in energy than a (2)-(1) configuration.[9] We find both the new (2)-(1) and (1)-(1)-(1) configurations mentioned above, with the new one being 0.05 eV/H lower in energy than the (1)-(1)-(1).

The most stable $\{I, H_4\}$ defect we found, shown in Fig. 7, is made up from the $\{I, H_3\}$ defect of Fig. 6 with a defect similar to the H_1^* adjacent to it at the antibonding-type site as shown by Chadi.[35] This $\{I, H_4\}$ defect has a (2)-(1)-(1) configuration and C_1 symmetry. Our $\{I, H_4\}$ defect is different from the lowest-energy one found by Hastings *et al.*[13] within HF theory, which has a (1)-(1)-(1)-(1) configuration. We have not been able to obtain the lowest-energy $\{I, H_4\}$ structure from Ref. 9, although from the description given, we know that it is different from ours. We are therefore unable to perform a full comparison of energies for $\{I, H_4\}$.

Information about the electronic structures of the defects can be obtained from the DFT energy levels. The hexagonal self-interstitial defect introduces a doubly-occupied level near the valence-band maximum (VBM) and a doubly-occupied level about 0.3 eV above the VBM. There are no further energy levels within the band gap. The C_{3v} symmetry $\{I, H_1\}$ defect is based on the hexagonal self-interstitial, and the lowest-energy H-derived level of $\{I, H_1\}$ lies within the conduction band, so this defect would tend to form a singly-

(a)   (b)
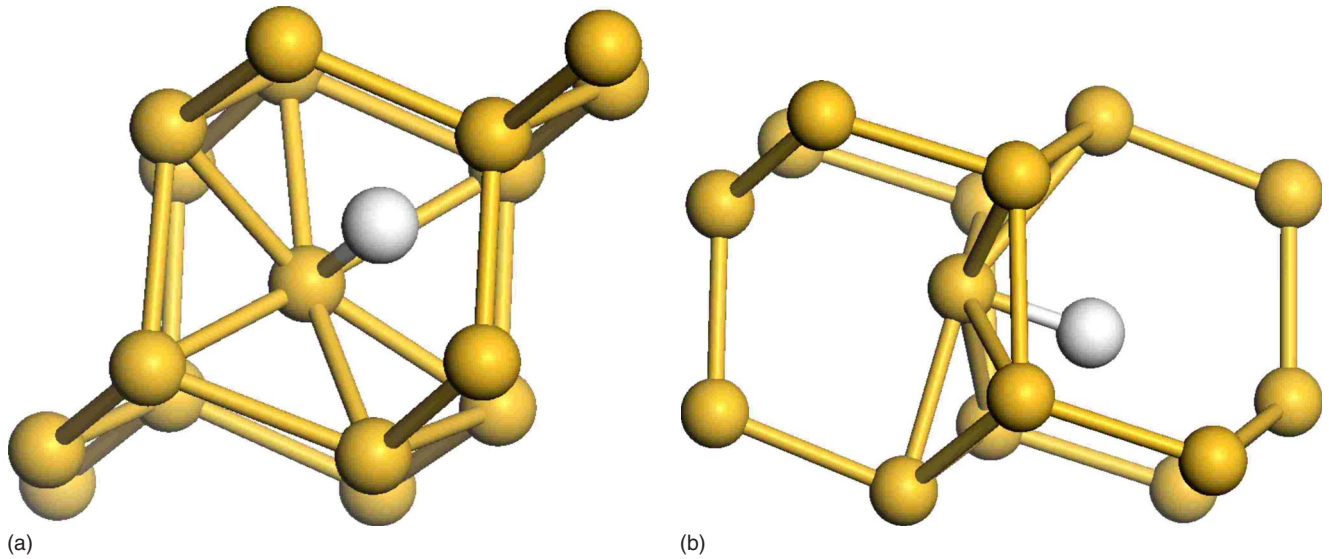
FIG. 3. (Color online) Two projections of the new $\{I,H\}$ defect of C_{3v} symmetry found in this work. Silicon atoms are shown in yellow (gray) and the hydrogen atom is white. This defect is based on a hexagonal self-interstitial rather than the split-$\langle 110 \rangle$ self-interstitial of previous work.

ionized state when the chemical potential lies between the gap levels and the conduction band. The C_1 symmetry $\{I,H_3\}$ defect has three doubly-occupied levels about 0.3 eV above the VBM, and a singly-occupied level lying within the conduction band. This defect would tend to form a singly-ionized state when the chemical potential lies between the gap levels and the conduction band. The most stable defects that we have found, the C_2 symmetry $\{I,H_2\}$ and the C_1 symmetry $\{I,H_4\}$ defects have doubly-occupied levels less than 0.3 eV above the VBM which accommodate all of the available electrons. These defects would tend to adopt neu-

tral charge states when the chemical potential lies above the gap levels. The $\{I,H_2\}$ and $\{I,H_4\}$ defects have fully saturated bonds while the $\{I,H_1\}$ and $\{I,H_3\}$ defects have unsaturated bonds, see Sec. V.
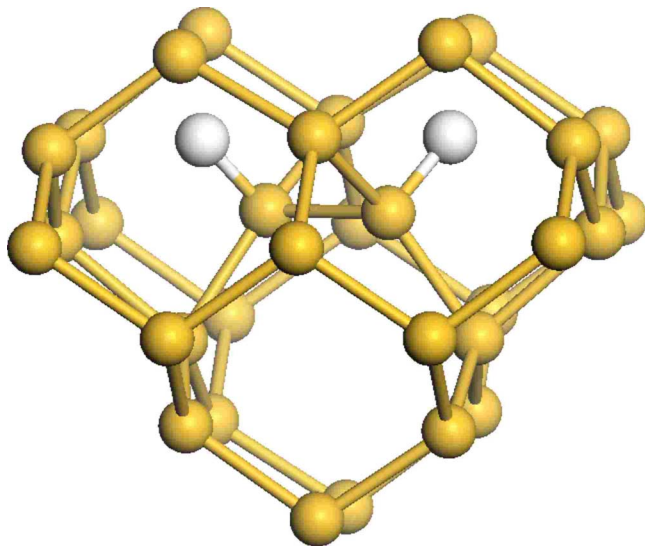
FIG. 4. (Color online) The most stable $\{I,H_2\}$ defect which has C_2 symmetry and was also found in previous work (Refs. 2 and 9–13). Silicon atoms are shown in yellow (gray) and the hydrogen atoms are white. The defect is based on a split-$\langle 110 \rangle$ silicon interstitial defect, with hydrogen atoms saturating the two dangling bonds.
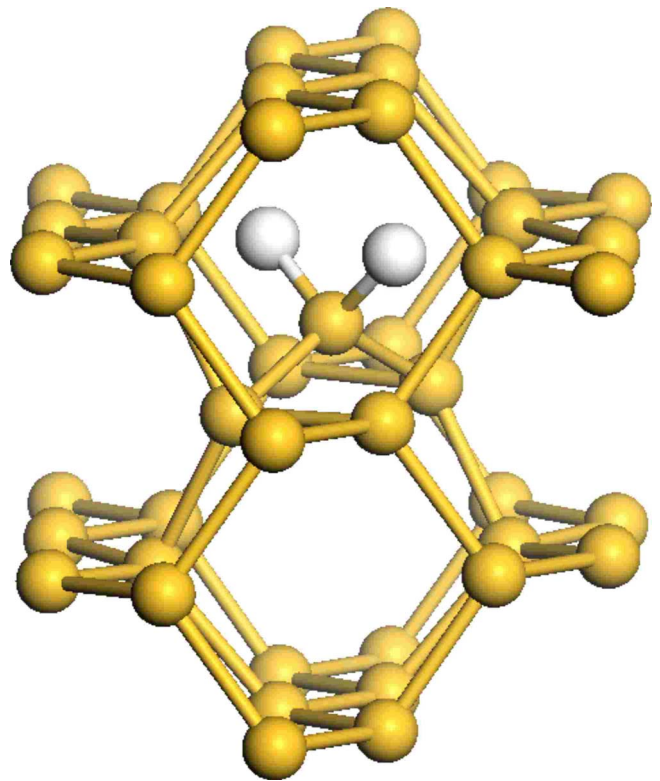
FIG. 5. (Color online) The second most stable $\{I,H_2\}^*$ defect which has C_2 symmetry and was also found in previous work (Ref. 10). Silicon atoms are shown in yellow (gray) and the hydrogen atoms are white. The defect is based on a buckled bond-centered silicon self-interstitial.
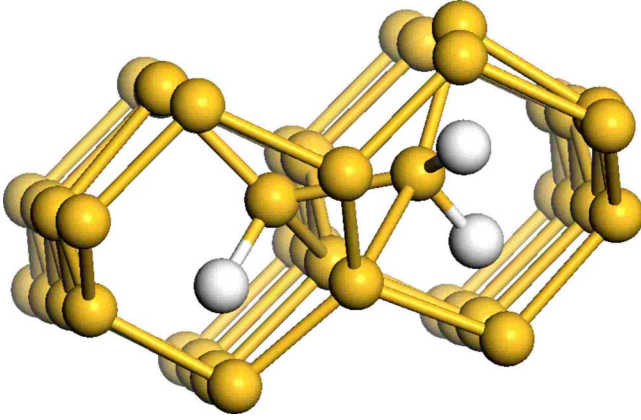
FIG. 6. (Color online) The new $\{I, H_3\}$ defect of C_1 symmetry found in this work. Silicon atoms are shown in yellow (gray) and the hydrogen atoms are white. The defect is based on a deformed split-$\langle 110 \rangle$ self-interstitial.

V. DISCUSSION

We have presented first-principles DFT results using random structure searching for hydrogen/silicon complexes in silicon. The searches were carried out in 32-atom silicon cells, while the final results were obtained with 256-atom cells. We used a multi-k-point generalization of the Baldereschi mean-value method to perform the BZ sampling, which we demonstrated to be superior to the standard MP sampling.

Formation energies of the defects were calculated with respect to the lowest-energy self-interstitial defect and
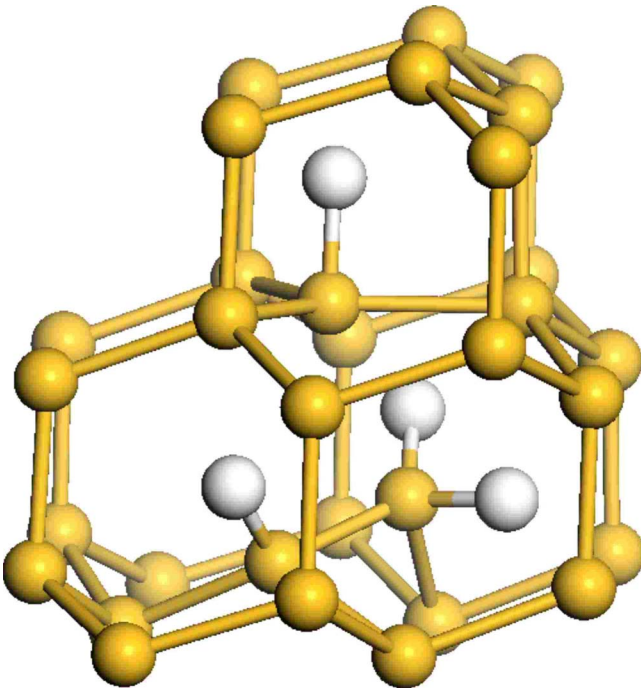
FIG. 7. (Color online) The new $\{I, H_4\}$ defect of C_1 symmetry found in this work. Silicon atoms are shown in yellow (gray) and the hydrogen atoms are white. It is based on the new $\{I, H_3\}$ (see Fig. 6) with a defect similar to the H_1^* defect of Chadi (Ref. 35) adjacent to it on the antibonding site.
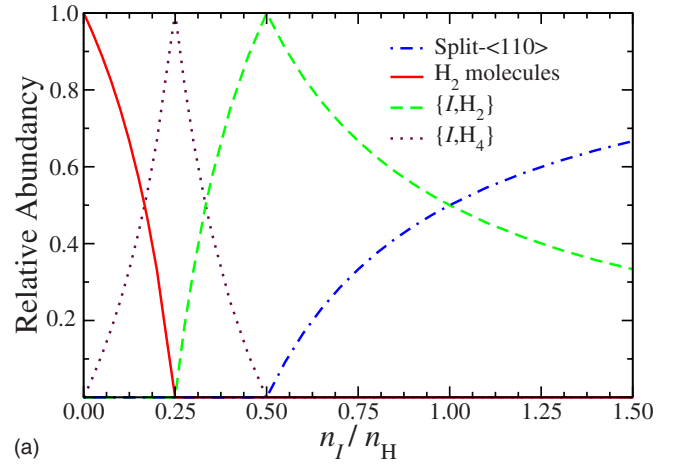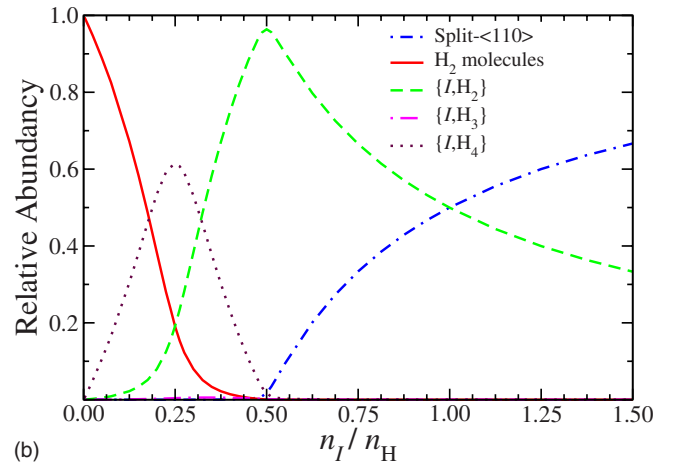
FIG. 8. (Color online) Relative abundances of the defects at (a) zero temperature and (b) 1200 K. n_I/n_H is the ratio of the concentration of interstitial silicon atoms to hydrogen atoms. At low n_I/n_H there is a large relative abundance of H_2 molecules. As n_I/n_H increases, H_2 molecules bind strongly to the Si self-interstitials, forming $\{I, H_4\}$ defects. As n_I/n_H increases further, formation of $\{I, H_2\}$ defects is favored. However, an increase in n_I/n_H above 0.5 does not lead to formation of $\{I, H\}$ because the mixed state of $\{I\}$ and $\{I, H_2\}$ is more favorable. The most significant differences at 1200 K are that the abundance of $\{I, H_4\}$ is somewhat reduced and that H_2 and $\{I, H_2\}$ defects are favored instead, and $\{I, H_3\}$ has a small but finite abundance in a region which peaks at around $n_I/n_H = 0.4$. The abundance of $\{I, H\}$ at 1200 K is negligible.

lowest-energy hydrogen defect in bulk silicon. We have confirmed that the previously described $\{I, H_2\}$ and $\{I, H_2\}^*$ defects are the most stable. We have, however, found a new $\{I, H\}$ defect which is significantly lower in energy than the one previously reported in the literature. Our defect is based on the hexagonal self-interstitial whereas the previously reported one was based on the split-$\langle 110 \rangle$ self-interstitial. We also found a new, lower-energy $\{I, H_3\}$ defect and a new $\{I, H_4\}$ defect.

The relative abundances of the defects at zero temperature can be calculated from the defect energies as a function of the ratio of the concentrations of the self-interstitial and hydrogen atoms, n_I/n_H. Figure 8(a) shows that only four defects can form in this model, ($\{I\}$, $\{I, H_2\}$, $\{I, H_4\}$, and $\{H_2\}$)

with the $\{I\}$ defect corresponding to the lowest-energy split-$\langle 110 \rangle$ self-interstitial. The main features of Fig. 8 are that when $n_I \ll n_H$ $\{I, H_4\}$ defects are formed and the surplus H atoms form $\{H_2\}$ defects, and when $n_I \gg n_H$ $\{I, H_2\}$ defects are formed and the surplus Si atoms form $\{I\}$ defects.

At finite temperatures [see Fig. 8(b)], we consider the defect free energies, which should contain contributions from the vibrational free energy and the configurational entropy. We have not evaluated the vibrational free energies, which would involve very costly phonon calculations, but we have calculated the configurational contributions. These are expected to be significant because we deal with defects containing from one atom (split-$\langle 110 \rangle$ self-interstitial) up to five atoms ($\{I, H_4\}$). In general, defects containing fewer atoms are expected to be favored by the configurational entropy at higher temperatures. The configurational entropy can be written in terms of the number of degenerate defect configurations per atomic site, d_i, where i labels the defect. The degeneracy d_i can be evaluated straightforwardly in some cases. For example, the $\{I, H\}$ defect of Fig. 3 has a degeneracy per atomic site of four because it is formed from a Si atom at a hexagonal site (of which there are two per atomic site), and the Si-H bond can point in one of two directions. Calculating the degeneracy for more complicated defects is not necessarily straightforward, and therefore we have developed a computational scheme to evaluate defect degeneracies. The scheme comprises the following steps:

(1) Generate a set of structures by applying the symmetry operations of the space group of the host crystal to the defect structure;

(2) Identify structures from this set which differ only by a translation vector of the lattice of the host crystal and remove all but one of them;

(3) The defect degeneracy per primitive unit cell is the number of structures remaining.

The defect degeneracies calculated in this fashion are reported in Tables II and III, where we present d_i only for the lowest-energy defect of each type. The defect concentrations are then obtained by minimizing the Helmholtz free energy of the system for fixed concentrations n_I and n_H. In our model we consider only the lowest-energy defects of each type listed in Tables II and III, and in a complete model other defects such as clusters of self-interstitial Si atoms and complexes involving other impurity atoms should be considered.

It is interesting to note that only the $\{I, H_2\}$, $\{I, H_2\}^*$, and $\{I, H_4\}$ defects are perfectly saturated, i.e., each Si atom has four covalent bonds and each H atom has one, and that these defects have the lowest total formation energies [defined as $nE_F(\{I, H_n\})$ with E_F given by Eq. (7)]. It is, of course, not possible to achieve perfect saturation of a Si/H structure with an odd number of H atoms, as such a structure would contain two bonds per Si atom and half a bond per H atom.

Overall we conclude that "random searching" is a useful tool for finding the structures of low-energy defects in semiconductors.

*ajm255@cam.ac.uk.

[1] C. G. Van de Walle and J. Neugebauer, Annu. Rev. Mater. Res. **36**, 179 (2006).

[2] M. Budde, B. B. Nielsen, P. Leary, J. Goss, R. Jones, P. R. Briddon, S. Öberg, and S. J. Breuer, Phys. Rev. B **57**, 4397 (1998).

[3] E. R. Batista, J. Heyd, R. G. Hennig, B. P. Uberuaga, R. L. Martin, G. E. Scuseria, C. J. Umrigar, and J. W. Wilkins, Phys. Rev. B **74**, 121102(R) (2006).

[4] R. J. Needs, J. Phys.: Condens. Matter **11**, 10437 (1999).

[5] S. Goedecker, T. Deutsch, and L. Billard, Phys. Rev. Lett. **88**, 235501 (2002).

[6] W.-K. Leung, R. J. Needs, G. Rajagopal, S. Itoh, and S. Ihara, Phys. Rev. Lett. **83**, 2351 (1999).

[7] B. N. Mukashev, K. A. Abdullin, and Y. V. Gorelkinskii, Phys. Status Solidi A **168**, 73 (1998).

[8] T. A. G. Eberlein, N. Pinho, R. Jones, B. J. Coomer, and J. Goss, Physica B **308-310**, 454 (2001).

[9] M. Gharaibeh, S. K. Estreicher, P. A. Fedders, and P. Ordejón, Phys. Rev. B **64**, 235211 (2001).

[10] P. Deák, M. Heinrich, L. C. Snyder, and J. W. Corbett, Mater. Sci. Eng., B **4**, 57 (1989).

[11] C. G. Van de Walle and J. Neugebauer, Phys. Rev. B **52**, R14320 (1995).

[12] P. Deák, L. C. Snyder, M. Heinrich, C. R. Ortiz, and J. W. Corbett, Physica B **170**, 253 (1991).

[13] J. L. Hastings, M. Gharaibeh, S. K. Estreicher, and P. A. Fedders, Physica B **273-274**, 216 (1999).

[14] C. J. Pickard and R. J. Needs, Phys. Rev. Lett. **97**, 045504 (2006).

[15] G. Csányi, C. J. Pickard, B. D. Simons, and R. J. Needs, Phys. Rev. B **75**, 085432 (2007).

[16] C. J. Pickard and R. J. Needs, Nat. Phys. **3**, 473 (2007).

[17] C. J. Pickard and R. J. Needs, J. Chem. Phys. **127**, 244503 (2007).

[18] C. J. Pickard and R. J. Needs, Phys. Rev. B **76**, 144114 (2007).

[19] C. J. Pickard and R. J. Needs, Nature Mater. **7**, 775 (2008).

[20] A. E. Mattsson, R. R. Wixom, and R. Armiento, Phys. Rev. B **77**, 155211 (2008).

[21] O. K. Al-Mushadani and R. J. Needs, Phys. Rev. B **68**, 235205 (2003).

[22] J. Shim, E.-K. Lee, Y. J. Lee, and R. M. Nieminen, Phys. Rev. B **71**, 245204 (2005).

[23] H. J. Monkhorst and J. D. Pack, Phys. Rev. B **13**, 5188 (1976).

[24] A. Baldereschi, Phys. Rev. B **7**, 5212 (1973).

[25] G. Rajagopal, R. J. Needs, S. Kenny, W. M. C. Foulkes, and A.

James, Phys. Rev. Lett. **73**, 1959 (1994).

[26] G. Rajagopal, R. J. Needs, A. James, S. D. Kenny, and W. M. C. Foulkes, Phys. Rev. B **51**, 10591 (1995).

[27] J. P. Perdew, K. Burke, and M. Ernzerhof, Phys. Rev. Lett. **77**, 3865 (1996).

[28] S. J. Clark, M. D. Segall, C. J. Pickard, P. J. Hasnip, M. I. J. Probert, K. Refson, and M. C. Payne, Z. Kristallogr. **220**, 567 (2005).

[29] D. Vanderbilt, Phys. Rev. B **41**, 7892 (1990).

[30] S. G. Louie, S. Froyen, and M. L. Cohen, Phys. Rev. B **26**, 1738 (1982).

[31] K. J. Chang and D. J. Chadi, Phys. Rev. B **40**, 11644 (1989).

[32] C. G. Van de Walle, Phys. Rev. B **49**, 4579 (1994).

[33] C. G. Van de Walle, Y. Bar-Yam, and S. T. Pantelides, Phys. Rev. Lett. **60**, 2761 (1988).

[34] C. G. Van de Walle, P. J. H. Denteneer, Y. Bar-Yam, and S. T. Pantelides, Phys. Rev. B **39**, 10791 (1989).

[35] D. J. Chadi, Appl. Phys. Lett. **83**, 3710 (2003).